Balanced vehicular traffic at a Bottleneck

Siebel, F., Moutari, S., Mauser, W., & Rascle, M. (2009). Balanced vehicular traffic at a Bottleneck. Mathematical and Computer Modelling, 49(3-4), 689-702.

Published in:
Mathematical and Computer Modelling

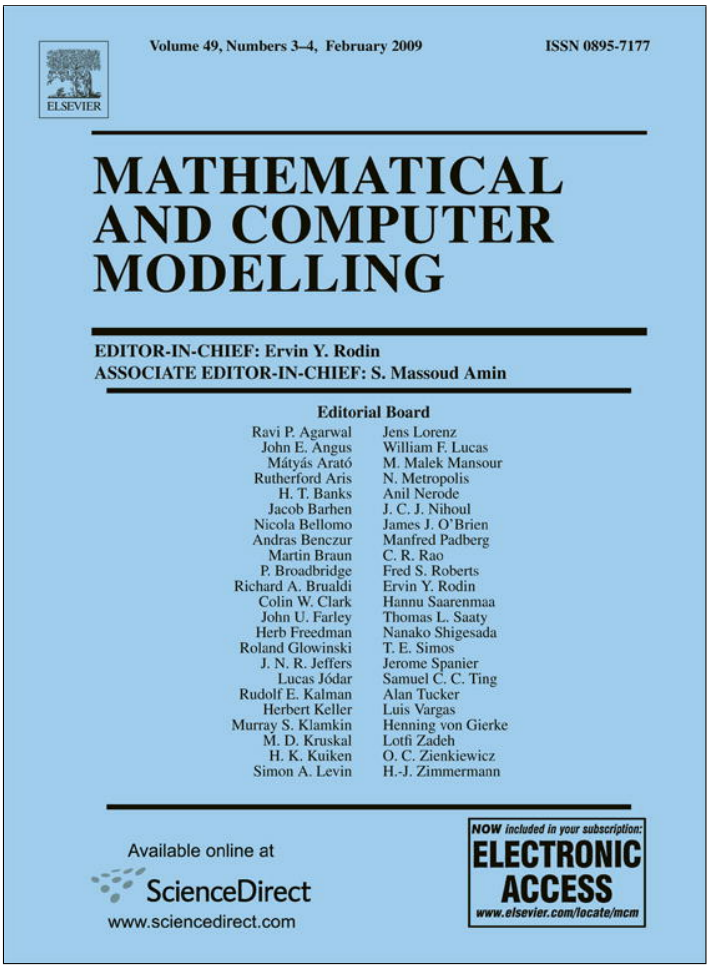

Available online at www.sciencedirect.com
ScienceDirect
Mathematical and Computer Modelling 49 (2009) 689–702
MATHEMATICAL AND COMPUTER MODELLING
www.elsevier.com/locate/mcm

Balanced vehicular traffic at a bottleneck

Florian Siebel[a,*], Wolfram Mauser[b], Salissou Moutari[c], Michel Rascle[c]

[a] *Sebastian-Andre-Weg 8, D-82362 Weilheim, Germany*
[b] *Department of Geography, University of Munich, Luisenstraße 37, D-80333 Munich, Germany*
[c] *Laboratoire J. A. Dieudonné, UMR CNRS N° 6621, Université de Nice-Sophia Antipolis, Parc Valrose, 06108 Nice Cedex 2, France*

Received 25 November 2007; accepted 24 January 2008

Abstract

The balanced vehicular traffic model is a macroscopic model for vehicular traffic flow. We use this model to study the traffic dynamics at highway bottlenecks either caused by the restriction of the number of lanes or by on-ramps or off-ramps. The coupling conditions for the Riemann problem of the system are applied in order to treat the interface between different road sections consistently. Our numerical simulations show the appearance of synchronized flow at highway bottlenecks.

Keywords: Macroscopic traffic model; Synchronized flow; Riemann problem; Highway bottleneck; Capacity drop

1. Introduction

The balanced vehicular traffic model [1] (BVT model) generalizes the macroscopic traffic model of Aw, Rascle [2,3] and Greenberg [4] by introducing an effective relaxation coefficient into the momentum equation of traffic flow. This effective relaxation coefficient can become negative, resulting in multivalued fundamental diagrams in the congested regime. Such negative effective relaxation coefficients follow from finite reaction and relaxation times of drivers [1]. For related ideas, see Greenberg–Klar–Rascle [5], Greenberg [6].

In a previous work [7] we studied the behavior of the BVT model at a bottleneck. There, we manipulated the partial differential equations describing traffic flow at the bottleneck by artificially resetting the average velocity in order to model a speed restriction. The results obtained in that study showed the basic behavior of the BVT model and its potential to explain the observed patterns of traffic flow [8] that were discussed (with other models [9,10]) elsewhere. Although the procedure of resetting quantities, i.e. the average velocity in that case, was locally restricted, it leaves the question whether the model can adequately describe synchronized flow at a bottleneck. In order to show this, the current paper systematically studies the traffic dynamics at highway bottlenecks in the BVT model by numerical means. To do this in agreement with the underlying partial differential equations, we use the coupling conditions for the Riemann problems at the interfaces between different highway sections. We focus the discussion on two setups:

* Corresponding author.
E-mail addresses: florian.siebel@gmx.de (F. Siebel), w.mauser@iggf.geo.uni-muenchen.de (W. Mauser), salissou@math.unice.fr (S. Moutari), rascle@math.unice.fr (M. Rascle).

0895-7177/$ - see front matter
doi:10.1016/j.mcm.2008.01.006

In the first setup we study a bottleneck caused by the narrowing of a highway from three lanes to two lanes. In the second setup we study a two-lane highway with an on-ramp and an off-ramp.

The outline of the paper is as follows. In Section 2 we summarize the theory of the coupling conditions for the Riemann problem at intersections. Whereas Section 3 presents numerical results for a highway bottleneck caused by the restriction of the number of lanes from three lanes to two lanes, Section 4 presents the numerical results for a two-lane highway with an on-ramp and an off-ramp. In Section 5 we introduce the possible generalization to an arbitrary junction. We finally summarize our results in Section 6.

2. Coupling conditions

Before we have a closer look at the coupling conditions, let us repeat the principal equations of the BVT model. The evolution equations for the density ρ of vehicles and the average velocity v are described by the following hyperbolic system of balance laws

$$\frac{\partial \rho}{\partial t} + \frac{\partial(\rho v)}{\partial x} = 0, \tag{2.1}$$

$$\frac{\partial(\rho(v - u(\rho)))}{\partial t} + \frac{\partial(\rho v(v - u(\rho)))}{\partial x} = b(\rho, v)\rho(u(\rho) - v). \tag{2.2}$$

Here, $u(\rho)$ denotes the equilibrium velocity, therefore the expression $v - u(\rho) = w$ describes a distance to equilibrium. The quantity $b(\rho, v)$ is the effective relaxation coefficient. For the case where $b(\rho, v)$ becomes negative, there are additional equilibrium velocities, i.e. high-flow branch and the jam line. Whereas the high-flow branch is metastable for intermediate densities and unstable for high densities, the jam line is unstable for intermediate densities and metastable for high densities [7]. The precise expressions of $u(\rho)$ and $b(\rho, v)$ are recalled in Section 3. Note that the pseudo-momentum $\rho(v - u(\rho))$ is not conserved due to the nonvanishing term on the right-hand side of Eq. (2.2). This source term plays an essential role for the traffic dynamics on road sections, but it is neglected for the situation where one is interested in the Riemann problems at intersections, since it is never a delta-function.

2.1. Background

Piccoli and Garavello [11] appear to have been the first to propose an intersection modeling by using the Aw–Rascle "second-order" model [2] of traffic flow. In their approach, only the mass flux is conserved but not the pseudo-momentum. Herty and Rascle [12] proposed another approach in which mass flux and pseudo-momentum are both conserved. But they maximized the mass fluxes at the intersection with some arbitrary *given* homogenization coefficients. The latter approach has been generalized by maximizing the total mass flux at the junction without fixing any condition [13]. In fact, the homogenization coefficients are not arbitrary but obtained directly from the mass flux maximization. Another approach is also based on the mass flux maximization [14,15]. Our approach in the current paper is similar to the latter one, in particular we maximize the total flux at the junction, at the same time we approximate properly the resulting pseudo-momentum of the original "Aw–Rascle" system on the outgoing roads. Here, we are particularly concerned with the BVT model [1]. We note that our treatment of the homogenization problem which naturally arises in a merge junction differs from earlier work [12,13], where the modeling is rigorously described from microscopic considerations, but it leads to formulas which are a bit more complex. Here our description of the coupling conditions is simpler and in practice is a good approximation of the previous ones, see Section 2.5.

2.2. Junction consisting of one incoming and one outgoing road

In the following we restrict the discussion to the Riemann problem at the interface between two road sections. The road section 1 is located upstream and the road section 2 downstream of the interface, where the flux functions have to be determined. Let $U_1^- = (\rho_1^-, \rho_1^- v_1^-)$ be the state vector at the interface upstream in the road section 1 and let $U_2^+ = (\rho_2^+, \rho_2^+ v_2^+)$ be the state vector at the interface downstream in the road section 2 (see panel (a) of Fig. 1). For each road section j we introduce the function w_j of the state variable $U = (\rho, \rho v)$

$$w_j(U) = v - u_j(\rho). \tag{2.3}$$

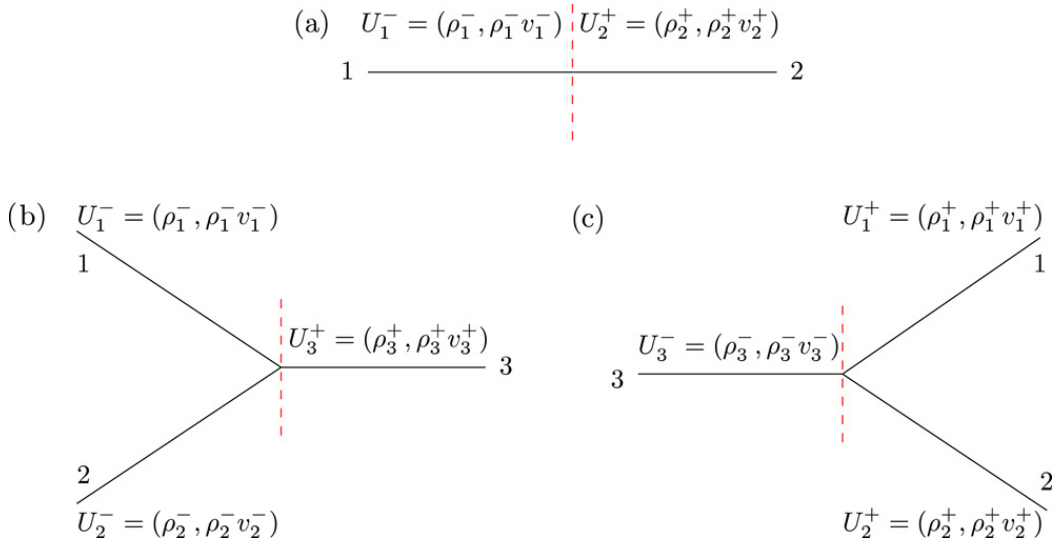

Fig. 1. Definition of the quantities at junctions, which are necessary to construct the boundary fluxes. The junction in (a) consists of one incoming and one outgoing road. The panels (b) and (c) display a merge junction and a diverge junction, respectively. The direction of the flow is from left to right.

According to Herty and Rascle [12] the fluxes at the interface between the two road sections (see Eqs. (2.1) and (2.2))

$$\hat{f} = q \begin{pmatrix} 1 \\ w_1(U_1^-) \end{pmatrix} \tag{2.4}$$

can be calculated from the expression

$$q = \min(d_1(\rho_1^-), s_2(\rho_2^\dagger)), \tag{2.5}$$

where the demand and supply functions $d_1(\rho)$ and $s_2(\rho)$ and the density $\rho_2^\dagger$ are defined below.

The density $\rho_2^\dagger$ is defined as the intersection point of the two curves $v = v_2^+$, $w_2(U) = w_1(U_1^-)$ and can be obtained by solving the implicit equation

$$u_2(\rho_2^\dagger) - v_2^+ + w_1(U_1^-) = 0. \tag{2.6}$$

Let us define the function

$$\eta_{d1}(\rho) = \rho u_1(\rho) + \rho w_1(U_1^-). \tag{2.7}$$

For a monotonously decreasing, differentiable function $u_1(\rho)$ the function $\eta_{d1}(\rho)$ has a single maximum at location $\tilde{\rho}_1$, which can be obtained by solving the implicit equation

$$\eta'_{d1}(\tilde{\rho}_1) = \tilde{\rho}_1 u'_1(\tilde{\rho}_1) + u_1(\tilde{\rho}_1) + w_1(U_1^-) = 0. \tag{2.8}$$

It is now possible to define the demand function[1]

$$d_1(\rho) = \begin{cases} \eta_{d1}(\rho), & \text{if } \rho \le \tilde{\rho}_1, \\ \eta_{d1}(\tilde{\rho}_1), & \text{if } \rho > \tilde{\rho}_1. \end{cases} \tag{2.9}$$

Let us define the function

$$\eta_{s2}(\rho) = \rho u_2(\rho) + \rho w_1(U_1^-). \tag{2.10}$$

[1] Note that in a previous work [16] we exchanged the terms demand and supply in comparison to the standard notation used here. The demand describes the maximum flow that the road section 1 can deliver to the road section 2.

For a monotonously decreasing, differentiable function $u_2(\rho)$ the function $\eta_{s2}(\rho)$ has a single maximum at location $\tilde{\rho}_2$, which is determined by solving the implicit equation

$$\eta'_{s2}(\tilde{\rho}_2) = \tilde{\rho}_2 u'_2(\tilde{\rho}_2) + u_2(\tilde{\rho}_2) + w_1(U_1^-) = 0. \tag{2.11}$$

With this function we define the supply function as

$$s_2(\rho) = \begin{cases} \eta_{s2}(\tilde{\rho}_2), & \text{if } \rho < \tilde{\rho}_2, \\ \eta_{s2}(\rho), & \text{if } \rho \geq \tilde{\rho}_2. \end{cases} \tag{2.12}$$

We numerically solve the implicit equations (2.8) and (2.11) using the method of nested intervals. With the expression for the fluxes at the interface between the two road sections (see Eq. (2.4)), we obtain the necessary boundary values at the interface for the conservative update scheme [1].

2.3. Merge junction

We are now interested in the boundary fluxes at a merge junction, see panel (b) of Fig. 1. In order to define the demand functions on the incoming road sections $i = 1, 2$ we first define the functions $\eta_{di}(\rho)$ as follows,

$$\eta_{di}(\rho) = \rho u_i(\rho) + \rho w_i(U_i^-). \tag{2.13}$$

Let us denote the maxima of the corresponding curves as $\tilde{\rho}_i$. We can then define the demand function of the road section i as

$$d_i(\rho) = \begin{cases} \eta_{di}(\rho), & \text{if } \rho \leq \tilde{\rho}_i, \\ \eta_{di}(\tilde{\rho}_i), & \text{if } \rho > \tilde{\rho}_i. \end{cases} \tag{2.14}$$

In order to define the supply function in the road section 3, we first introduce quantities β_i describing the fraction of cars entering from the road section i into the road section 3. When we assume that the incoming fluxes passing through the junction are proportional to the incoming demands, we have

$$\beta_i = \frac{d_i(\rho_i^-)}{\sum_{j=1}^{2} d_j(\rho_j^-)}. \tag{2.15}$$

With this definition, we follow the work of Haut and Bastin [14,15] and do not consider these fractions as part of the optimization problem [13]. We define the homogenized value w_3^* for the quantity w defined in Eq. (2.3), i.e.

$$w_3^* = \sum_{j=1}^{2} \beta_j w_j(U_j^-), \tag{2.16}$$

and with the latter the function

$$\eta_{s3}(\rho) = \rho u_3(\rho) + \rho w_3^* \tag{2.17}$$

which reaches its maximum value at $\tilde{\rho}_3$.

We are now able to define the supply function

$$s_3(\rho) = \begin{cases} \eta_{s3}(\tilde{\rho}_3), & \text{if } \rho < \tilde{\rho}_3, \\ \eta_{s3}(\rho), & \text{if } \rho \geq \tilde{\rho}_3. \end{cases} \tag{2.18}$$

This function will be evaluated below at the intersection point of the two curves $v = v_3^+$ and $w_3(U) = w_3^*$, which corresponds to a density $\rho_3^\dagger$ fulfilling the implicit equation

$$u_3(\rho_3^\dagger) - v_3^+ + w_3^* = 0. \tag{2.19}$$

Finally, we define the downstream boundary fluxes in the road section i as

$$\hat{f}_i^- = q\beta_i \begin{pmatrix} 1 \\ w_i(U_i^-) \end{pmatrix} \tag{2.20}$$

and the upstream boundary fluxes in the road section 3 as

$$\hat{f}_3^+ = q \begin{pmatrix} 1 \\ w_3^* \end{pmatrix}, \tag{2.21}$$

where

$$q = \min\left(\sum_{j=1}^{2} d_j(\rho_j^-), s_3(\rho_3^\dagger)\right). \tag{2.22}$$

Note that the above boundary fluxes are conserved through the intersection, and are bounded from above by the demands and supplies.

2.4. Diverge junction

In this section we study the boundary fluxes at a diverge junction, see panel (c) of Fig. 1. Again we set

$$\eta_{d3}(\rho) = \rho u_3(\rho) + \rho w_3(U_3^-) \tag{2.23}$$

and denote the maximum of that function as $\tilde{\rho}_3$. The demand function in the road section 3 is defined as

$$d_3(\rho) = \begin{cases} \eta_{d3}(\rho), & \text{if } \rho \le \tilde{\rho}_3, \\ \eta_{d3}(\tilde{\rho}_3), & \text{if } \rho > \tilde{\rho}_3. \end{cases} \tag{2.24}$$

For the definition of the supply function we first have to prescribe the fractions of cars intending to enter from road section 3 into road section 1 and road section 2, which we describe with the quantities α_{31} and α_{32}. We stress that these quantities – in contrast to the work of Haut and Bastin [14,15] – need not agree with the actual percentages of the flow from road section 3 entering into road section 1 and road section 2, see Eqs. (2.31)–(2.34). Under the assumption that all cars remain in the network, i.e. $\alpha_{31} + \alpha_{32} = 1$, we can set

$$\alpha_{31} = \alpha, \tag{2.25}$$

$$\alpha_{32} = (1 - \alpha), \tag{2.26}$$

with $\alpha \in [0, 1]$. For the outgoing road sections $k = 1, 2$ we define

$$\eta_{sk} = \rho u_k(\rho) + \rho w_3(U_3^-) \tag{2.27}$$

and denote the maxima of these functions $\tilde{\rho}_k$. The supply function on the outgoing road section k then reads

$$s_k(\rho) = \begin{cases} \eta_{sk}(\tilde{\rho}_k), & \text{if } \rho < \tilde{\rho}_k, \\ \eta_{sk}(\rho), & \text{if } \rho \ge \tilde{\rho}_k. \end{cases} \tag{2.28}$$

We also have to determine the densities $\rho_k^\dagger$, at which these supply functions are evaluated. These densities are calculated from the intersection of the curves $v = v_k^+$ and $w_k(U) = w_3(U_3^-)$, which reduces to the implicit equations

$$u_k(\rho_k^\dagger) - v_k^+ + w_3(U_3^-) = 0. \tag{2.29}$$

Finally, we define the downstream boundary fluxes of road section 3 as

$$\hat{f}_3^- = q \begin{pmatrix} 1 \\ w_3(U_3^-) \end{pmatrix} \tag{2.30}$$

and the upstream boundary fluxes in road section 1 as

$$\hat{f}_1^+ = q_1 \begin{pmatrix} 1 \\ w_3(U_3^-) \end{pmatrix}, \tag{2.31}$$

and in the road section 2 as

$$\hat{f}_2^+ = q_2 \begin{pmatrix} 1 \\ w_3(U_3^-) \end{pmatrix}, \tag{2.32}$$

where

$$q_1 = \min\left(\alpha d_3(\rho_3^-), s_1(\rho_1^\dagger)\right), \tag{2.33}$$

$$q_2 = \min\left((1-\alpha) d_3(\rho_3^-), s_2(\rho_2^\dagger)\right), \tag{2.34}$$

and

$$q = q_1 + q_2. \tag{2.35}$$

Note again that the above boundary fluxes are conserved through the interface, and are bounded from above by the demands and supplies.

2.5. Comparison to earlier work

In this section we compare the above treatment of the coupling conditions to earlier approaches [12–15].

The approach of Haut and Bastin [14,15] differs from our approach in the treatment of a diverge junction. Using our notation the percentage of the flow $\tilde{\alpha}$ which enters from section 3 into section 1 is fixed in the work of Haut and Bastin [14,15]. Instead of Eqs. (2.33)–(2.35) the optimization problem reduces to

$$q_1 = \tilde{\alpha} q, \tag{2.36}$$

$$q_2 = (1-\tilde{\alpha}) q, \tag{2.37}$$

and

$$q = \min\left(d_3(\rho_3^-), \frac{s_1(\rho_1^\dagger)}{\tilde{\alpha}}, \frac{s_2(\rho_2^\dagger)}{1-\tilde{\alpha}}\right). \tag{2.38}$$

As a consequence of this treatment, if only one of the outgoing roads is jammed up, the outflow of the other road will be zero as well.

The approach taken in the work of Herty, Moutari and Rascle [12,13] differs from our approach in the treatment of a merge junction. Whereas we take the homogenization coefficients β_i proportional to the respective demands (see Eq. (2.15)), the quantities are either fixed [12] or considered as part of the optimization problem [13]. Moreover, in Eq. (2.17) we assume that the velocity on road 3, near the junction, is given by $v = u_3(\rho) + w_3^*$. This is in contrast with the work of Herty, Moutari and Rascle [12,13], where the mixture of cars from both incoming roads 1 and 2 is assumed to produce a *homogenized* flow, with a nonlinear relation between ρ and v which expresses that the cars from roads 1 and 2 microscopically share the available space. The resulting mixture rule is more appropriately described in Lagrangian (mass) coordinates, but is definitely *not* in the above form.

In other words, rigorously speaking, the assumptions of Herty, Moutari and Rascle [12,13] are incompatible with the (simpler) formula (2.17), which we use here. In practice the latter is a good approximation of the former since the difference is not necessarily significant. We will come back to this point elsewhere.

3. Lane reduction on a highway

We study the traffic dynamics for the setup depicted in Fig. 2. The highway under study consists of two 7 km long road sections. The road section 1 consists of three lanes whereas the road section 2 consists of two lanes. Note that in

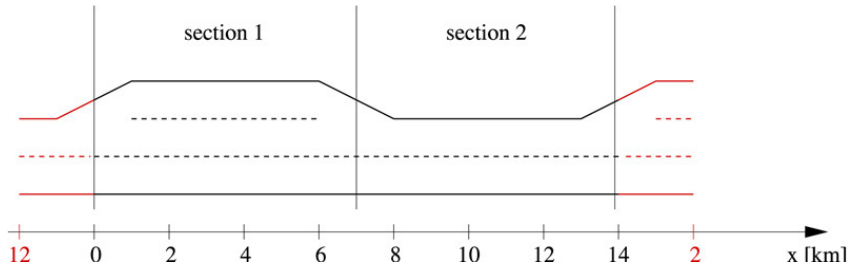

Fig. 2. Sketch of the highway under study. The highway consists of two road sections of 7 km length. The road section 1 consists of three lanes whereas the road section 2 consists of two lanes. We use periodic boundary conditions, i.e. the road section 1 is also located downstream of the road section 2.

the mathematical description the transition from two to three lanes is immediate, the length of the merging segments is neglected. We further prescribe periodic boundary conditions. Hence, the evolution is fully determined by the initial data on the two road sections. As in our previous work [7] we use the equilibrium velocity function of Newell

$$u(\rho) = u_m \left(1 - \exp\left(-\frac{\lambda}{u_m}\left(\frac{1}{\rho} - \frac{1}{\rho_m}\right)\right)\right) \tag{3.1}$$

with parameter values $u_m = 160$ km/h, $\lambda = 3600$ (1/h/lane), $\rho_m = 160$ (1/km/lane) and an effective relaxation coefficient

$$b(\rho, v) = \begin{cases} \dfrac{a_c}{u - v}, & \text{if } \tilde{\beta}(\rho, v)(u(\rho) - v) - a_c \geq 0, \\ \dfrac{d_c}{u - v}, & \text{if } \tilde{\beta}(\rho, v)(u(\rho) - v) - d_c \leq 0, \\ \tilde{\beta}(\rho, v), & \text{else}, \end{cases} \tag{3.2}$$

$$\tilde{\beta}(\rho, v) = \frac{1}{\hat{T} u_m} \left(|u(\rho) - v + a_1 \Delta v| + a_2 \Delta v\right) \tag{3.3}$$

and

$$\Delta v(\rho) = \tanh\left(a_3 \frac{\rho}{\rho_m}\right)\left(u(\rho) + c\rho_m\left(\frac{1}{\rho} - \frac{1}{\rho_m}\right)\right), \tag{3.4}$$

with parameters $a_c = 2$ m/s^2, $d_c = -5$ m/s^2, $\hat{T} = 0.1$ s, $a_1 = -0.2$, $a_2 = -0.8$, $a_3 = 7$ and $c = -14$ km/h. Thus the maximum density of the road section 1 is 480 vehicles/km. The road section 2 can support 320 vehicles/km at maximum. The initial data to start the numerical simulations consist of equilibrium data on the two road sections. We prescribe a constant vehicle density ρ_0 in both road sections, setting the initial velocity to $v = u(\rho_0)$. We choose the constant ρ_0 to be independent of the number of the lanes, the corresponding scaled densities in each road section follow from dividing ρ_0 by the number of lanes of that road section.

3.1. Parameter study

In the following we perform a parameter study of ρ_0, varying the quantity between 50 (1/km) and 300 (1/km) in steps of 50 (1/km). Fig. 3 displays the simulation results for the density (left column) and velocity (right column) for simulations covering two hours. Note that, although the initial data are in equilibrium in each road section, the coupling conditions at the interface between the two road sections do not guarantee the equilibrium during the evolution.

For a density $\rho_0 = 50$ (1/km), a small region of higher density and lower velocity forms between about 5.5 km and 7 km. This region corresponds to data located in the fundamental diagram on and scattered around the jam line. Clearly, this congested region is fixed at the bottleneck and therefore cannot correspond to a wide moving jam. The structure is supported by the bottleneck, i.e. the insufficient capacity of the road section 2 to carry the corresponding free-flow rates in the road section 1. This region corresponds to synchronized flow. For a density $\rho_0 = 100$ (1/km), the dynamics becomes more complicated, but finally a synchronized flow region of extended width (ranging from about 2 km to 7 km) forms. Only in a small region of the road section 1 (between 0 km and 2 km) traffic is in free

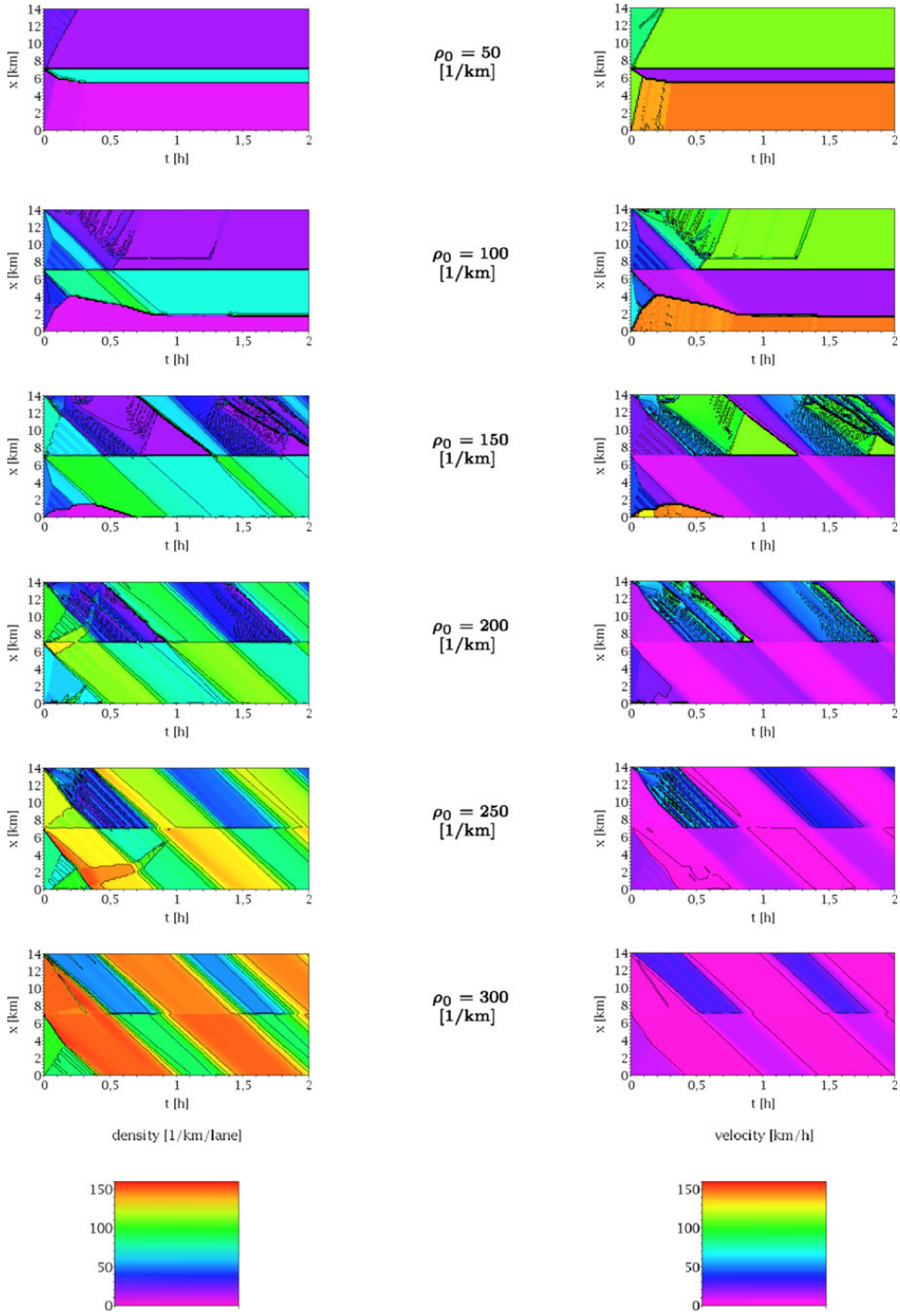

Fig. 3. Traffic dynamics at the bottleneck caused by the reduction of the number of lanes on a highway. The column on the left shows the evolution of the vehicle density in units (1/km/lane), the column on the right the corresponding evolution of the velocity in units (km/h). The different rows correspond to different simulation runs varying the initial density $\rho = \rho_0$ as indicated. See the text for a detailed description.

flow. For a density $\rho_0 = 150$ (1/km), the synchronized flow region covers the entire road section 1. Moreover, a wide moving jam travels through the two road sections, see the bright pink structure in the velocity plot. Increasing the density still further leads to even wider wide moving jams. The velocities inside these jams decrease with the increase of the initial density ρ_0. For $\rho_0 = 300$ (1/km) velocities of less than 1 (km/h) are reached inside the wide moving jam. Note that the wide moving jams are not affected by the interfaces between the two road sections of the highway. They travel upstream with an almost constant speed.

3.2. Static solutions

In order to obtain a better understanding on the appearance of synchronized flow in front of the bottleneck we study static solutions for the setup. Steady-state solutions are found for an appropriate coordinate system $(\tilde{t}, z) = (t, x - \hat{w}t)$, when all time derivatives with respect to $\tilde{t}$ vanish [7]. Here, the speed $\hat{w}$ is a constant. It follows from (2.1) and (2.2) that steady-state solutions fulfill the following set of equations [7][2]

$$q = \rho(v - \hat{w}), \tag{3.5}$$

$$\frac{\mathrm{d}v}{\mathrm{d}z} = \frac{b(\rho, v)(u(\rho) - v)}{v + \rho u'(\rho) - \hat{w}}, \tag{3.6}$$

with a constant flow q. From these equations we derive an ordinary differential equation for the density of steady-state solutions,

$$\frac{\mathrm{d}\rho}{\mathrm{d}z} = \frac{\rho^2}{q} \frac{b(\rho, v)(\rho\hat{w} + q - \rho u(\rho))}{q + u'(\rho)\rho^2}. \tag{3.7}$$

For static solutions, moreover, we have $\hat{w} = 0$ and $z = x$.

Having a closer look at the results in Fig. 3 for initial densities $\rho_0 = 50$ (1/km) and $\rho_0 = 100$ (1/km), we observe that the dynamics finally settles and a static solution forms.

In the following we will analyze these static solutions in more detail. The upper and lower left panels of Fig. 4 display the density and flow profiles, for the initial density $\rho_0 = 50$ (1/km) as well as for an initial density of $\rho_0 = 100$ (1/km). We note that apart from the location of the shock discontinuity, which is located at about 5.5 km and about 1.8 km respectively, the solutions are identical. The upper right panel of Fig. 4 displays the solution for $\rho_0 = 50$ (1/km) in the flow-density-diagram. In addition we indicated for each highway section the equilibrium flow curve $\rho u(\rho)$ and the additional equilibrium curves, which correspond to the zeros of the effective relaxation coefficient $b(\rho, v)$, i.e. the high-flow branch and the jam line. As a result of our previous work [7], these curves can be subdivided into stable, metastable and unstable branches, which are shown as solid, dashed and dotted curves in this figure. Moreover, the numerical fluxes at the interface between grid cells in our conservative evolution scheme are constant over the entire domain, and correspond to a flow $q = 3743$(1/h).

Shock discontinuities have to fulfill the Rankine–Hugoniot jump conditions, which are given in our system by

$$0 = (\rho v)_R - (\rho v)_L, \tag{3.8}$$

$$0 = (\rho v(v - u(\rho)))_R - (\rho v(v - u(\rho)))_L. \tag{3.9}$$

Here the subscripts L and R denote the states left and right of the shock. Eq. (3.8) expresses the conservation of the vehicle number flow. The second Rankine–Hugoniot jump condition (3.9) reduces to $(v - u(\rho))_R = (v - u(\rho))_L$. For the state on the left (upstream) of the shock we have $v = u(\rho)$. Hence, this condition has to be fulfilled for the state on the right of the shock (downstream) as well. As the state on the right is an unstable equilibrium state, the solution settles to the metastable jam line corresponding to the same flow value. Up to numerical errors, the observed transition layer is reproduced by the static solution (3.7) with $\hat{w} = 0$. At the interface between sections 1 and 2 at 14 km, which corresponds – due to the periodic boundary condition – also to 0 km, the coupling condition $(v - u_2(\rho))_R = (v - u_1(\rho))_L$ is trivially fulfilled, as both states are in equilibrium in their particular section. At the interface between sections 1 and 2 at 7 km, we can determine the coupling conditions by solving the following implicit equation for the density ρ_R on the right in section 2

$$\frac{v_L \rho_L}{\rho_R} - u_2(\rho_R) = v_L - u_1(\rho_L). \tag{3.10}$$

The corresponding state $(\rho_R, \rho_R v_R)$ is located above the jam line in the fundamental diagram (see the upper right panel of Fig. 4). Hence, in order to link this state with the stable free-flow section corresponding to the same flow value, the solution has to cross the jam line. This is only possible provided that the denominator on the right-hand

[2] Note that the correct equation (15) of this reference should be $x = z + w\tilde{t}$.

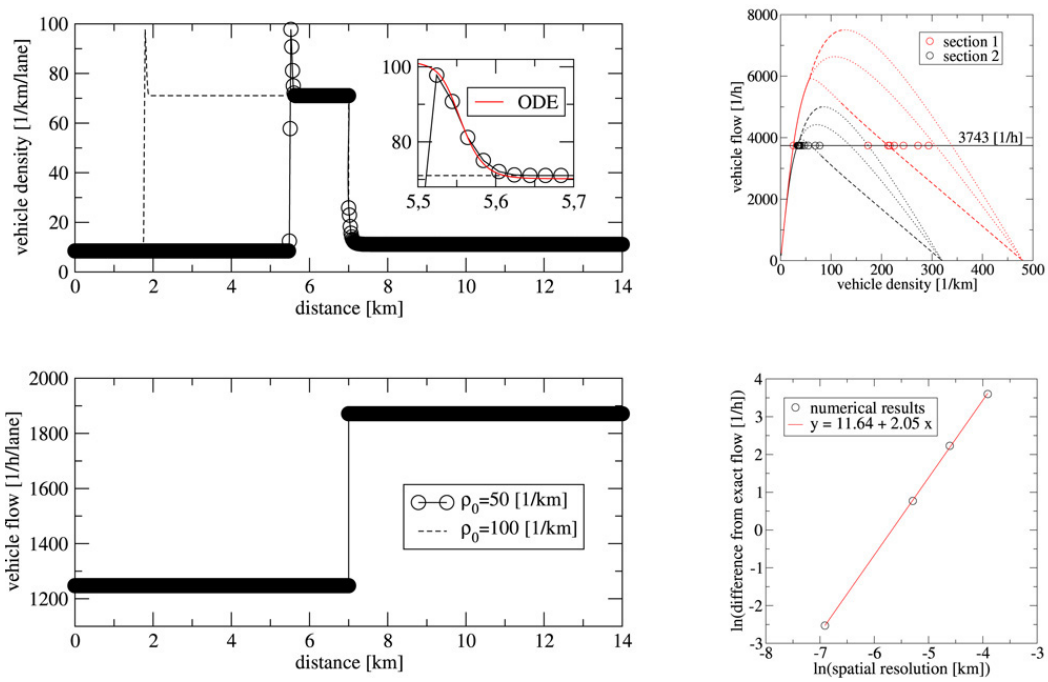

Fig. 4. Static solution with synchronized flow in front of the bottleneck, which is caused by the reduction of the number of lanes from 3 in section 1 (0–7 km) to 2 in section 2 (7–14 km). The two panels on the left show the vehicle density and flow profiles for the static solutions, which finally form for an initial density $\rho_0 = 50$ (1/km) (solid line with circles) and $\rho_0 = 100$ (1/km) (dashed line). Up to the location of the shock discontinuity, the static solution is independent of the initial data. Note that for the vehicle flow, the two curves for initial density $\rho_0 = 50$ (1/km) and $\rho_0 = 100$ (1/km) fully overlap. We further stress that the peaks located at about 5.5 km for $\rho_0 = 50$ (1/km) and at about 1.8 km for $\rho_0 = 100$ (1/km) in the upper left panel correspond to sections of nontrivial static solutions. This can be seen in the inset of the upper left panel, where we showed for comparison the solution of the ordinary differential equation (3.7). The situation in the flow-density-diagram is shown in the upper right panel, where the circles correspond the the static data for $\rho_0 = 50$ (1/km). Moreover, we added the equilibrium curves for each highway section, that is the curves $\rho u(\rho)$ and the high-flow branch and the jam line, which correspond to zeros of the effective relaxation coefficient $b(\rho, v)$. The sections of equilibrium curves are plotted as solid (dashed, dotted) lines corresponding to whether sections are stable (metastable, unstable). The static solution corresponds to a constant flow of 3743 (1/h). The lower right panel shows the difference of the theoretical value for the constant flow 3779.80 (1/h) of static solutions and the numerical value obtained for different resolutions. Using a double-logarithmic scale, the data points are well fitted by a straight line with a slope of about two, which is expected for the application of a second-order numerical scheme.

side of Eq. (3.7) vanishes on the jam line. The numerator trivially vanishes, as $b(\rho, v) = 0$ on the jam line. Suppose, the denominator has a finite value. Then, the derivate $\mathrm{d}\rho/\mathrm{d}z$ would change sign at the jam line, and it would not be possible to construct a decreasing function $\rho(z)$, which is necessary to reach a state on the free-flow branch. Note that a similar discussion applies to the existence of wide cluster solutions in some different traffic models described by systems of balance laws [17,18]. Setting the denominator on the right-hand side of Eq. (3.7) to zero, we obtain an implicit equation for the density ρ_c at the intersection with the jam line

$$v^j(\rho_c) + \rho_c u'(\rho_c) = 0. \tag{3.11}$$

Here, the velocity on the jam line, which corresponds to $b(\rho, v) = 0$, can be calculated from

$$v^j(\rho) = u(\rho) + (a_1 + a_2)\Delta v(\rho). \tag{3.12}$$

The solution of Eq. (3.11) gives

$$\rho_c = 57.32 \text{ (1/km)}, \tag{3.13}$$

and the corresponding flow value is

$$q = \rho_c v^j(\rho_c) = 3779.80 \text{ (1/h)}. \tag{3.14}$$

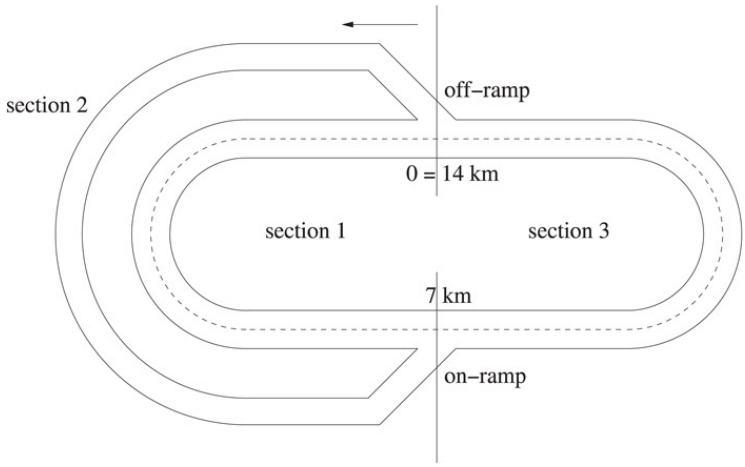

Fig. 5. Sketch of the simulation setup. We study the dynamics on a two-lane highway with an on-ramp between the road Sections 1 and 3 at 7 km (bottom of the picture) and an off-ramp between the road Sections 1 and 3 at $0 = 14$ km (top of the picture). For simplicity, we do not represent the simulation results on road section 2, but we will use the incoming and outgoing fluxes on this road section to compute the results on road Sections 1 and 3, i.e. on- and off-ramp form the boundaries of the one-lane road section 2.

This value is different from the numerical value of the flow in the right upper panel of Fig. 4, where we observed a value of 3743 (1/h). However, this difference is only a consequence of discretization errors for the numerical solution, the numerical value approaches the theoretical value with increasing resolution, the convergence rate being, as expected, two. This can be seen in the lower right panel of Fig. 4.

Experimental data for highway bottlenecks caused by a lane drop show a largely constant outflow [19] with values of up to about 1800 (1/h/lane) for the British motorway M4, which is close to our observed value of 1890 (1/h/lane). Of course, this value strongly depends on the specific situation in each country and is determined by the precise choice of the parameter values of the equilibrium velocity curve $u(\rho)$ and the effective relaxation coefficient $b(\rho, v)$ within the model. It is expected that we overestimate the flow value, as we did not account for trucks in our model. However, the numerical results are capable of reproducing the experimental fact, that the outflow downstream of a lane drop bottleneck on a highway is constant and significantly lower than the maximum of free flow in that section. This experimental observation follows within the BVT model from the necessary conditions for static solutions to form at the bottleneck.

4. Bottlenecks caused by on-ramps and off-ramps

In the second setup we analyze by numerical means a two-lane highway with an on-ramp and an off-ramp. The simulation setup is displayed in Fig. 5. For our simulations we chose a length of 7 km for two-lane road sections 1 and 3 each, and a length of 10 km for the one-lane road section 2. For the parameterization of the equilibrium velocity curve and the effective relaxation coefficient, we use again the values given in Eqs. (3.1)–(3.4). We start the simulations with a constant density in equilibrium on all road sections of $\rho_0 = 50$ (1/km/lane) and vary the percentage of cars α aiming to enter the road section 1 from the road section 3, see Eq. (2.25). The numerical results are summarized in Fig. 6. For small to intermediate values of the parameter α, the simulations develop a state, where the road section 1 is almost empty, i.e. traffic is in free flow in the road section 1. This can be easily understood by realizing that for small values of α most of the cars use the by-pass road section 2. In contrast, traffic is in the congested regime in the road section 3. For sufficiently high values of α (see the results for $\alpha = 0.5$) synchronized flow develops in front of the on-ramp in the road section 1. For $\alpha = 0.7$ there is only a small region of free flow remaining in road section 1 which disappears after a time of about 0.8 h. For a parameter value $\alpha = 0.9$ a region of narrow moving jams forms in front of the off-ramp in the road section 3.

5. Extension to a general junction

For a given junction n, let us denote by δ_n^- and δ_n^+, respectively the set of all incoming roads to n (indexed i in what follows) and the set of all the outgoing roads to n (indexed k in the following). We require the Eqs. (2.1) and

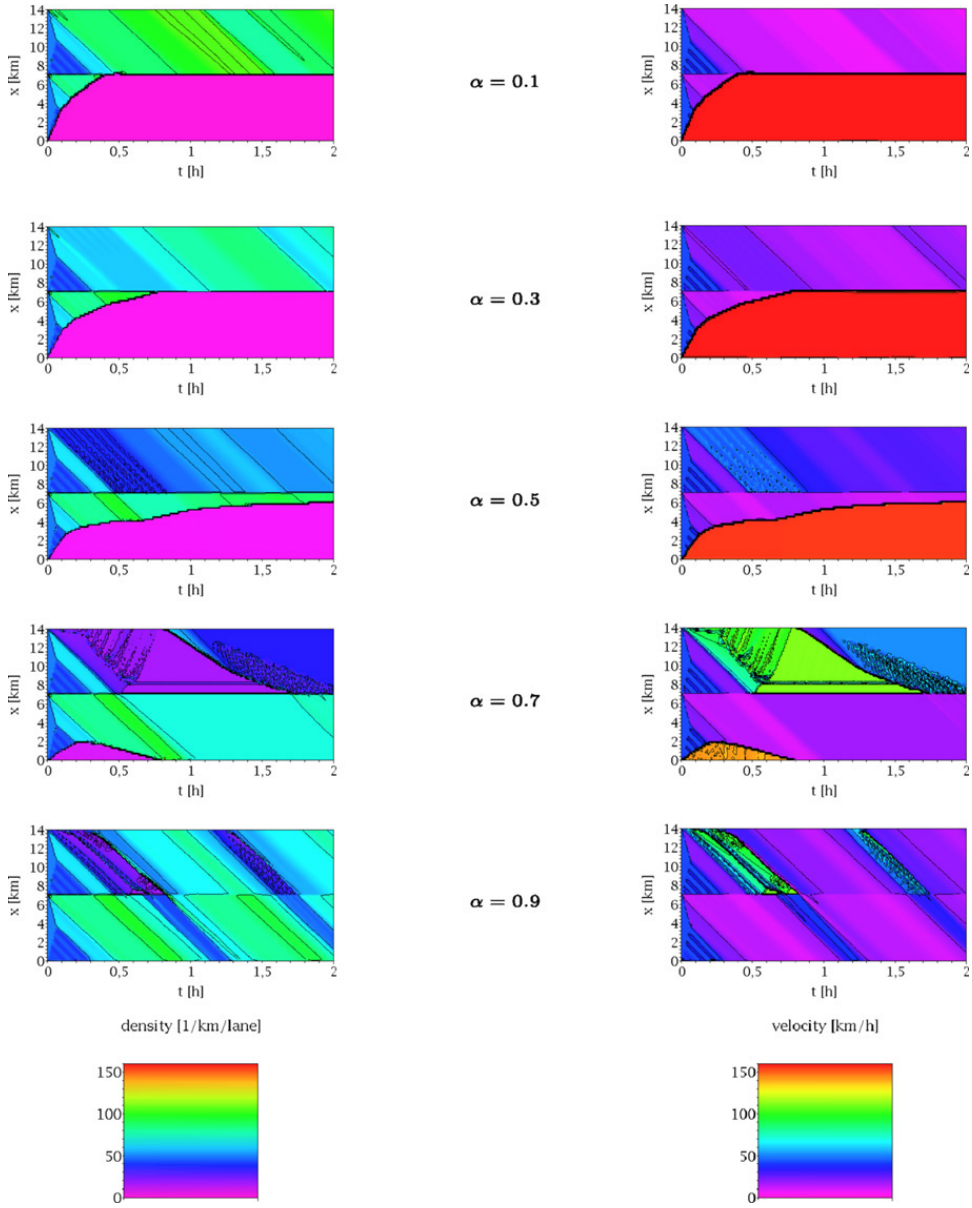

Fig. 6. Traffic dynamics at highway bottlenecks caused by on-ramps and off-ramps. The plot shows the traffic dynamics on the two-lane highway, the road section 1 corresponds to the region between 0 and 7 km, the road Section 3 corresponds to the region between 7 and 14 km. We vary the percentage of cars intending to enter from the road Section 3 into the road section 1, i.e. the value of α, in the range between 0.1 and 0.9 (different rows). The column on the left shows the evolution of the vehicle density in units (1/km/lane), the column on the right the corresponding evolution of the velocity in units (km/h).

(2.2) to hold on each road of $\delta_n^- \cup \delta_n^+$. The percentage of cars on the road i intending to go to the road k are denoted by α_{ik}, such that $\forall i \in \delta_n^-$, $\sum_k \alpha_{ik} = 1$. These coefficients are assumed to be known.

Let $U_i^- = (\rho_i^-, \rho_i^- v_i^-), \forall i \in \delta_n^-$ and $U_k^+ = (\rho_k^+, \rho_k^+ v_k^+), \forall k \in \delta_n^+$, respectively the boundary values on the incoming and outgoing roads. We denote by β_{ik}, such that $\forall k \in \delta_n^+$, $\sum_i \beta_{ik} = 1$, the portion of cars on the road k coming from the road i. We set

$$\beta_{ik} = \frac{\alpha_{ik} d_i(\rho_i^-)}{\sum\limits_{i \in \delta_n^-} \alpha_{ik} d_i(\rho_i^-)} \quad \forall i \in \delta_n^-,\ \forall k \in \delta_n^+, \tag{5.1}$$

with the demand functions d_i as defined in Eqs. (2.13) and (2.14). The homogenized w on the outgoing roads near the junction are as follows

$$w_k^* = \sum_{i \in \delta_n^-} \beta_{ik} w_i(U_i^-), \quad \forall k \in \delta_n^+. \tag{5.2}$$

With these quantities we define the supply functions s_k as in Eqs. (2.17) and (2.18) for arbitrary $k \in \delta_n^+$. For all $k \in \delta_n^+$, the intermediate state of density $\rho_k^\dagger$ on the outgoing road is given by the intersection point between the curves $v_k(U) = v_k^+$ and $w_k(U) = w_k^*$.

To obtain the flux q on each road one has to solve the following maximization problem

$$\max \sum_{k \in \delta_n^+} q_k \text{ subject to} \tag{5.3a}$$

$$0 \le q_i \le d_i(\rho_i^-), \quad \forall i \in \delta_n^-; \tag{5.3b}$$

$$0 \le q_k \le s_k(\rho_k^\dagger), \quad \forall k \in \delta_n^+; \tag{5.3c}$$

$$q_i = \sum_{k \in \delta_n^+} \beta_{ik} q_k, \quad \forall i \in \delta_n^-; \tag{5.3d}$$

$$q_k \le \sum_{i \in \delta_n^-} \alpha_{ik} d_i(\rho_i^-), \quad \forall k \in \delta_n^+. \tag{5.3e}$$

6. Conclusion

We have studied the balanced vehicular traffic model at highway bottlenecks caused by the reduction of the number of lanes and the effects of an on-ramp and an off-ramp. To this aim we performed numerical simulations changing the initial density and the routing parameter at the off-ramp respectively. For the lane reduction setup the numerical results show that already for moderate densities, synchronized flow forms at the bottleneck. The width of the synchronized flow region increases with increasing density. At the same time, the outflow from the bottleneck stays constant, with a flow value below the maximum capacity of the downstream road section, thus reproducing a capacity drop. This is a consequence of the conditions for static solutions. For large densities, wide moving jams appear which travel with a constant velocity upstream. Wide moving jams are not affected by the interface between the highway sections, i.e. by a change in the number of lanes on the highway. For the setup with an on-ramp and an off-ramp our numerical simulation shows that synchronized flow can form upstream of the on-ramp, but also in front of an off-ramp, where narrow moving jams can emerge.

The theory of the coupling conditions described in this paper can be applied to the balanced vehicular traffic model at a general junction, thus guaranteeing the conservation of the fluxes in the corresponding Riemann problems at intersections.

Acknowledgments

F. Siebel would like to thank the Laboratoire J. A. Dieudonné at Université Nice Sophia-Antipolis for the support and hospitality.

This work has been partially supported by the French ACI-NIM (Nouvelles Interactions des Mathématiques) No 193 (2004).

References

[1] F. Siebel, W. Mauser, On the fundamental diagram of traffic flow, SIAM Journal on Applied Mathematics 66 (4) (2006) 1150–1162.
[2] A. Aw, M. Rascle, Resurrection of "second order" models of traffic flow, SIAM Journal on Applied Mathematics 60 (3) (2000) 916–938.
[3] H.M. Zhang, A non-equilibrium traffic model devoid of gas-like behavior, Transportation Research B 36 (2002) 275–290.
[4] J.M. Greenberg, Extensions and amplifications of a traffic model of Aw and Rascle, SIAM Journal on Applied Mathematics 62 (3) (2001) 729–745.
[5] J.M. Greenberg, A. Klar, M. Rascle, Congestion on multilane highways, SIAM Journal on Applied Mathematics 63 (3) (2002) 818–833.
[6] J.M. Greenberg, Congestion redux, SIAM Journal on Applied Mathematics 64 (4) (2004) 1175–1185.
[7] F. Siebel, W. Mauser, Synchronized flow and wide moving jams from balanced vehicular traffic, Physical Review E 73 (6) (2006) 066108.

[8] B. Kerner, The Physics of Traffic, Springer, Berlin, 2004.
[9] D. Helbing, M. Treiber, Critical discussion of synchronized flow, Cooperative Transportation Dynamics 1 (2002) 2.1–2.24.
[10] M. Treiber, A. Kesting, D. Helbing, Delays, inaccuracies, and anticipation in microscopic traffic models, Physica A 360 (1) (2006) 71–88.
[11] M. Garavello, B. Piccoli, Traffic flow on a road network using the Aw–Rascle model, Communications in Partial Differential Equations 31 (2) (2006) 243–275.
[12] M. Herty, M. Rascle, Coupling conditions for a class of "second-order" models for traffic flow, SIAM Journal on Mathematical Analysis 38 (2) (2006) 595–616.
[13] M. Herty, S. Moutari, M. Rascle, Optimization criteria for modelling intersections of vehicular traffic flow, Networks and Heterogeneous Media 1 (2) (2006) 275–294.
[14] B. Haut, G. Bastin, A second order model for road traffic networks, in: Proceedings of the 8th International IEEE Conference on Intelligent Transportation Systems, 2005, pp. 178–184.
[15] B. Haut, G. Bastin, A second order model of road junctions in fluid models of traffic networks, Networks and Heterogeneous Media 2 (2) (2007) 227–253.
[16] F. Siebel, W. Mauser, Simulating vehicular traffic in a network using dynamic routing, Mathematical and Computer Modelling of Dynamical Systems 13 (1) (2007) 83–97.
[17] P. Zhang, S.C. Wong, Essence of conservation forms in the traveling wave solutions of higher-order traffic flow models, Physical Review E 74 (2) (2006) 026109.
[18] P. Zhang, S.C. Wong, S.-Q. Dai, Characteristic parameters of a wide cluster in a higher-order traffic flow model, Chinese Physics Letter 23 (2) (2006) 516–519.
[19] R. Bertini, M. Leal, Empirical study of traffic features at a freeway lane drop, Journal of Transportation Engineering 131 (12) (2005) 397–407.